

S²AG-Vid: Enhancing Multi-Motion Alignment in Video Diffusion Models via Spatial and Syntactic Attention-Based Guidance

Yuanhang Li^{1,2}, Qi Mao^{1*}, Lan Chen¹, Zhen Fang¹, Lei Tian²,
Xinyan Xiao², Libiao Jin¹, Hua Wu²

¹Communication University of China, Beijing, China ²Baidu Inc., Beijing, China
{qimao, yuanhangli, faziizhen, libiao}@cuc.edu.cn chenlaneva@mails.cuc.edu.cn
{tianlei09, xiaoxinyan, wu_hua}@baidu.com

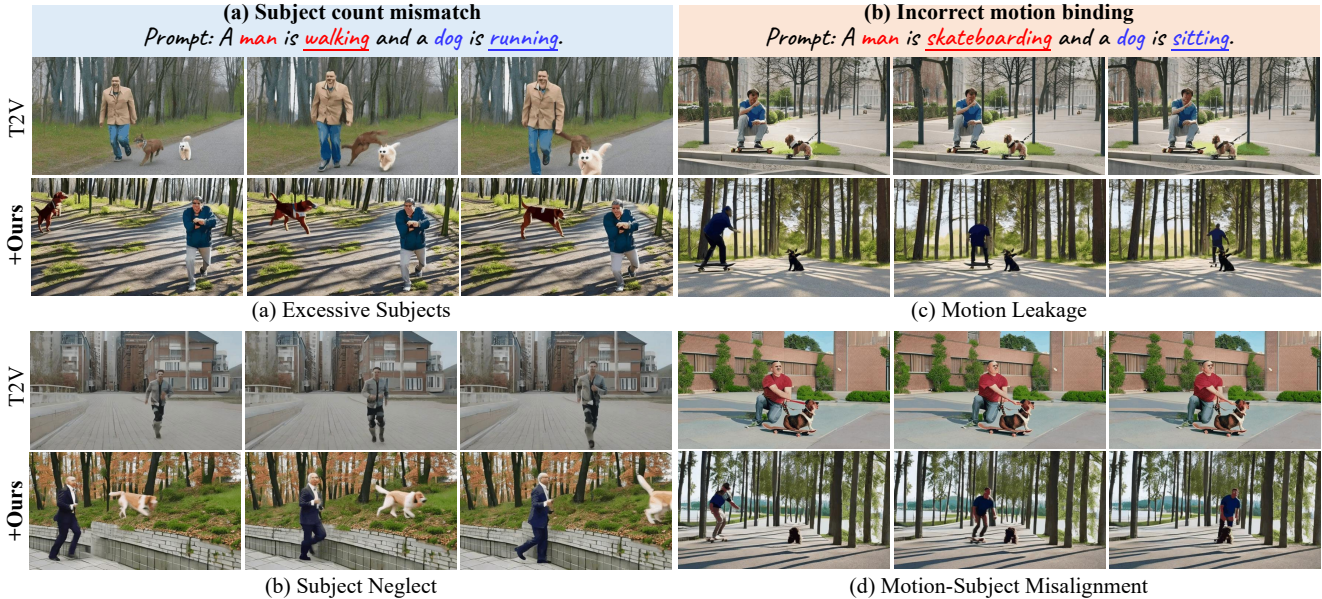


Figure 1. **Failure cases of open-source U-Net based text-to-video (T2V) diffusion models.** In scenarios involving multiple subjects with distinctive motions, the generated videos do not always align well with the textual descriptions, resulting in subject count mismatches and incorrect motion binding issues. Our approach, S²AG-Vid, incorporates both spatial and syntax-aware attention guidance to enhance the alignment of multiple subjects and their respective motions.

Abstract

Recent advancements in text-to-video (T2V) generation using diffusion models have garnered significant attention. However, existing T2V models primarily focus on simple scenes featuring a single object performing a single motion. Challenges arise in scenarios involving multiple objects with distinct motions, often leading to incorrect video-text alignment between subjects and their corresponding motions. To address this challenge, we propose S²AG-Vid, a training-free inference-stage optimization method that improves the alignment of multiple objects with their corresponding motions in T2V models. S²AG-Vid initially applies a spatial position-based, cross-attention (CA) constraint in the early stages of the denoising process, facilitating multiple nouns distinctly attending to the correct subject regions. To enhance the motion-subject binding, we implement a

syntax-guided contrastive constraint in the subsequent denoising phase, aimed at improving the correlations between the CA maps of verbs and their corresponding nouns. Both qualitative and quantitative evaluations demonstrate that the proposed framework significantly outperforms baseline approaches, producing higher-quality videos with improved subject-motion consistency.

1. Introduction

In recent years, significant progress has been made in diffusion-based text-to-image (T2I) generation models [21, 23, 25], enabling the creation of visually high-quality images that correspond closely to the provided text prompts. Expanding upon this achievement, researchers have broadened the scope of diffusion models to encompass text-to-video (T2V) generation [4, 12, 28, 32]. Existing T2V generation models primarily focus on simple scenes featuring a *single* object with a *single* motion. However, when users express the need for more expansive scenarios involving *multiple* objects with *distinct* motions, these models (de-

*Corresponding Author
Preliminary version, in progress.

noising network based on UNet[24] or DIT[18]) increasingly encounter the issue of prompt unfollowing, where the generated videos are not faithful to the semantics of the text prompts. The main obstacle in this regard is the incorrect alignment between the subjects and their corresponding motions.

We have identified two common issues of incorrect motion correspondence in open-source text-to-video (T2V) generation models, such as ModelScope [28]. Consider the prompt “*a man is walking and a dog is running*”, as illustrated in Fig. 1. Current models often struggle to accurately comprehend the number of subjects in the prompt, causing the **subject count mismatch** issue. Consequently, the generated video may sometimes include a man and two or more dogs (Fig. 1 (a), excessive subjects), while in other instances, it may only include a man (Fig. 1(b), subject neglect). The difficulty in generating the appropriate number of subjects leads to discrepancies in motion correspondence within the video, which deviates from the provided textual description. Furthermore, even when the correct number of subjects is identified, accurately associating motion with the corresponding subject remains challenging, i.e., **incorrect motion binding**. For instance, when provided with the prompt “*A man is skateboarding and a dog is sitting*”, the resulting video may exhibit both the man and dog skateboarding (Fig. 1(c), motion leakage), or show the man standing while the dog is skateboarding (Fig. 1(d), motion-subject misalignment).

To address the aforementioned challenges, our initial focus is on demonstrating that the cross-attention (CA) maps of verbs in T2V diffusion models can effectively capture the spatial trajectory of motions. Subsequently, we make two key observations towards CA maps of both nouns and verbs on video-text misalignment and alignment examples using ModelScope [28]: First, the CA maps corresponding to subject nouns fail to converge within defined areas in the early denoising timestep, lacking clear differentiation from one another. This, in turn, obstructs the concentration of high-attention areas of verbs into specific regions. Second, the CA maps associated with verbs struggle to accurately pinpoint the regions where their corresponding subjects are situated, thereby leading to issues such as motion leakage and inbinding. Consequently, an effective solution requires the **distinctly localization of the CA maps for nouns and the subsequent alignment of these maps with the CA maps of their corresponding verbs**.

Previous studies on T2I models have demonstrated some success in enhancing the CA map alignment of generated images with text descriptions by the introduction of spatial position-based priors [13, 14, 29, 34] and employing well-designed constraints to guide latent optimization [2, 6, 8, 11]. However, the issue of subject-motion misalignment has not been well studied in T2V generations. In this paper,

we introduce a novel inference-stage optimization method, termed **S²AG-Vid**, a training-free, plug-and-play approach that effectively bridges this gap by enforcing the alignment between multiple motions and their corresponding objects in T2V models. Based on the above two observations, we specifically design two cross-attention (CA)-based constraints that address both spatial and syntactic dimensions. During the early stage of denoising, we implement a spatial position-based prior to guiding the CA maps of nouns and verbs toward distinct and specific locations. In the subsequent denoising phase, we establish a syntax-guided contrastive constraint. This constraint aims to reduce the distance between the CA maps of verbs and their corresponding nouns relative to other words, thereby strengthening the association between subjects and their motions. Fig. 1 shows the effectiveness of the proposed method against T2V baselines, which significantly improves multi-motion alignment with their corresponding objects.

Our contributions can be summarized as follows:

- We propose a straightforward yet effective training-free approach to improve multi-motion correspondence in existing T2V diffusion models. To the best of our knowledge, this is the first attempt to tackle multiple subject-motion misalignment issues in T2V generation.
- We introduce spatial-aware and syntax-aware attention-based constraints, which are designed to direct motion focus towards the appropriate subject regions.
- Extensive quantitative and qualitative experiments demonstrate the effectiveness of our proposed method against other baselines using the benchmark with multiple subjects and diverse motions.

2. Related work

Text-to-Video Diffusion Models. Recently, diffusion-based T2V generation models [26, 28, 32, 33] have achieved significant progress. Several existing studies [10, 12, 33] have primarily focused on improving the temporal consistency of generated videos. For example, InstructVideo [33] enhances models through human feedback, whereas AnimateDiff [10] maintains fixed pre-training weights and updates only the motion modeling module. Additionally, some studies introduce [7, 15, 16, 31, 35] additional conditions such as depth maps [35], bounding boxes [16, 30], and motion trajectories [7, 31] to control the shape and movement of the video subjects. However, most existing research concentrates on scenarios featuring a single object performing a single motion. The complexities associated with multiple objects executing multiple motions remain underexplored. The issue of prompt unfollowing, such as incorrect video-text alignment between subjects and their corresponding motions, increasingly emerges in these complex settings.

Attention-Based Latent Guidance. Recent advances [2,

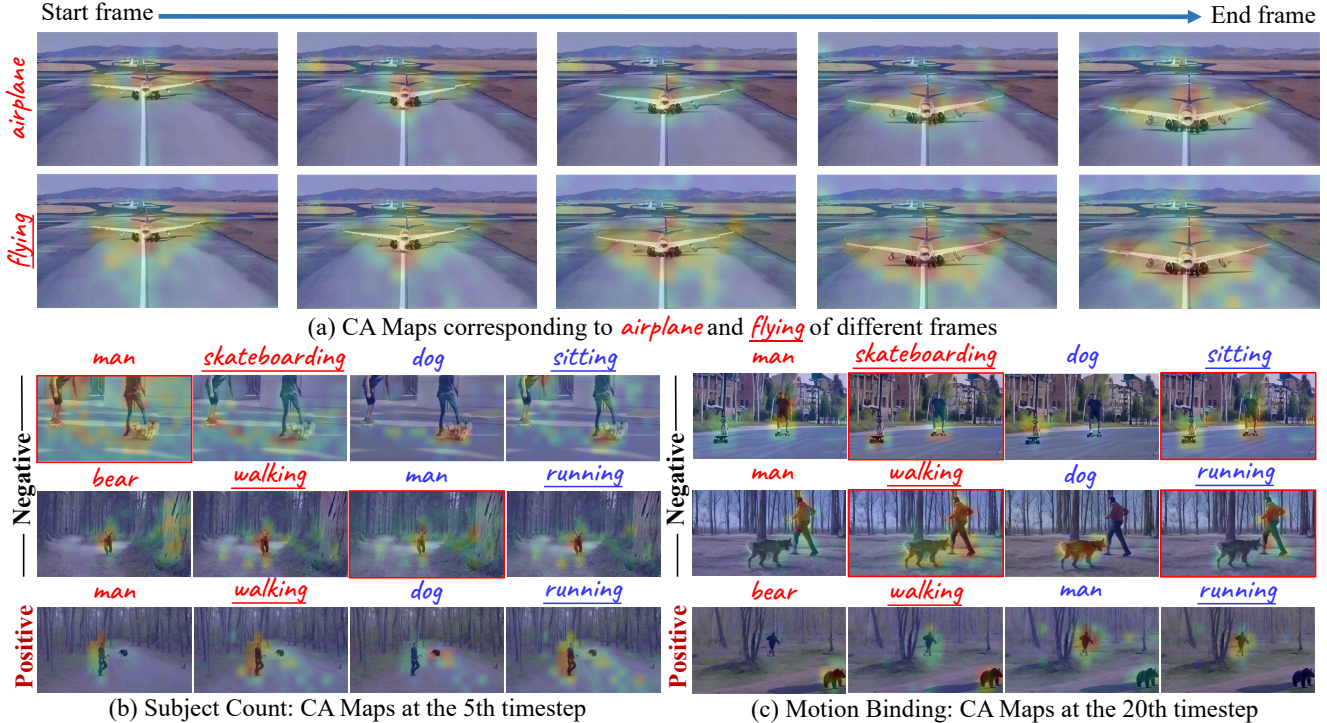


Figure 2. **Visualization of CA maps of nouns and verbs using ModelScope [28].** (a) The spatial trajectory of “*flying*” is effectively captured by the CA maps and correlates with shifts in the CA maps of the noun “*airplane*”. (b) During visualization, we examine examples of video-text misalignment (denoted as negative) and alignment (denoted as positive). In the early stage of denoising, we observe that the high-attention areas of nouns either overlap or are globally dispersed, resulting in instances of subject neglect and subject increase. (c) The CA map of the verb fails to align with the CA map of the noun, leading to motion leakage and incorrect binding.

5, 19, 22, 29] in T2I generation with diffusion models have investigated the use of CA constraints to optimize the noise latent feature during inference. Several works focus on addressing the prompt unfollowing issues in T2I generation. Attend-and-Excite [2] designs a loss function that directly adjusts the attention value of nouns to solve the problem of subject neglect in image generation. SynGen [22] adopts the linguistic structure of prompts to address issues of subject neglect and attribute leaks in image generation. Other line of works [6, 8, 17, 29] introduce additional spatial priors to control subject locations. Box-diff [6, 29] uses bounding boxes to constrain the subject’s CA maps. Meanwhile, some studies [8, 17] utilize masks to confine the focus CA maps’ areas and address attribute leakage in image generation and editing. Recent advancements in T2V generation [3, 15] also incorporate spatial priors using attention-based guidance to manage object motions. However, the issue of multiple subject-motion misalignment in T2V generation has not been thoroughly explored, which is the primary focus of this paper.

3. Methodology

In this section, we first discuss the rationale for enhancing motion correspondence through CA map adjustments, as detailed in Section 3.1. We then analyze the underlying causes of *subject count mismatch* and *incorrect motion*

binding by visualizing the CA maps of nouns and verbs, comparing successful video-text alignment (positive examples) and misalignment (negative examples) using Modelscope [28] in Section 3.2. This analysis leads to two key observations that motivate us to develop spatial-aware (Section 3.3.1) and syntax-aware (Section 3.3.2) attention-based constraints to improve multiple subject-motion correspondence.

3.1. Why Adjust the CA Map?

Let a T2V model generate a video $v \in F \times H \times W \times C$, where H, W, F and C indicate the height, width, number of frames and number of channels., respectively. The backbone diffusion models, typically employing a U-Net architecture, include two core modules that influence video motion: the temporal attention (TA) layer and the cross-attention (CA) layer within the spatial module. Within this framework, the CA layer integrates the input text information with the frame features. In this section, we analyze and explain why our focus is on adjusting the CA maps in the spatial module rather than the TA layer.

Temporal Attention. In the TA layer, $Q \in R^{N \times F \times d}$ and $K \in R^{N \times F \times d}$ are both intermediate visual features (d is the length of the query and key features). Then, the shape of the resulting TA map is $[N, F, F]$. $A_{p,q}^i$ of TA represents the correlation between the p -th frame and the q -th frame

of pixel i . Therefore, the TA maps focus exclusively on the similarity of pixel i across each frame, primarily enhancing inter-frame consistency without directly connecting to text prompts.

CA of the Spatial Module. The query feature $Q \in R^{F \times N \times d}$ ($N = h \times w$, $h \ll H$ and $w \ll W$) is the intermediate visual feature, the key $K \in R^{L \times d}$ (L is the number of words in the text prompt) is the text embedding, and the shape of the CA map is $[F, N, L]$. $A_{i,j}^f \in A$ represents the correlation between i -th pixel and j -th word in frame f . By visualizing the CA map, we can observe the area where the text prompt influences frame f . As demonstrated in Fig. 2(a), we visualize both the CA map of the noun “*airplane*” and the verb “*flying*” in the video frame. It can be clearly observed that the spatial trajectory of “*flying*” is effectively represented by the CA map and correlates with shifts in the CA map of the noun “*airplane*”. Consequently, by controlling the spatial position and trajectory of the CA maps for verbs and establishing a connection with the CA maps of nouns, we can influence the associated motions of the objects.

3.2. Motivations

As discussed in Section 3.1, the CA maps of verbs roughly capture the spatial trajectory of the motion. To better understand the increasing occurrences of *subject count mismatch* and *incorrect motion binding*, we first conduct experiments using Modelscope [28] with text descriptions that include two objects and two distinctive motions via the template “*a object1 is motion1 and a object2 is motion2*”. Next, we visualize CA maps of each noun and verb at different denoising timesteps by comparing successful video-text alignment (positive examples) and misalignment (negative examples). In Fig. 2(b) and Fig. 2(c), we focus on subject count and motion binding, respectively.

Observation 1: *The CA maps of nouns related to different objects are separate and focus on distinctive regions, which ensures the convergence of subjects into correct numbers.*

The early stages of the denoising phase in the T2V generative model typically establish the overall layout of the objects. As depicted in the first two rows of Fig. 2(b), at the 5-th denoising timestep, the highly correlated regions within the noun’s CA map do not rapidly converge to their corresponding areas nor do they separate effectively. Consequently, the number of subjects fails to align with the text description, leading to a mismatch between the motion in the generated video and the intended subject. As illustrated in the last row of Fig. 2(b), the areas of high attention on the noun’s CA map are relatively focused, and the nouns are distinctly separated, resulting in the accurate generation of the correct number of subjects.

Observation 2: *Ensuring strong connections between CA maps of verbs and nouns helps enhance motion corre-*

spendence.

As illustrated in the first two rows of Fig. 2(c), although by the 20-th denoising timestep, while the negative examples show that high-attention areas on the CA maps for nouns align with the corresponding objects, the CA maps for verbs still fail to accurately target the correct objects. This leads to motion leakage and incorrect binding. One potential reason is the use of the CLIP text encoder, known for its inability to effectively encode linguistic structures [9], resulting in a lack of clear relationship between verbs and nouns, and thus misalignment in the CA maps between verbs and their corresponding objects. However, as demonstrated in the positive example of Fig. 2(c), the CA map for the verb focuses solely on the appropriate subject area, ensuring that the subject’s motion is in accordance with the text description. Consequently, when the CA map of the verb closely mirror those of the corresponding noun, they facilitate accurate motion alignment.

3.3. Our Solution: S²AG-Vid

In this paper, we aim to enhance the multiple subjects and motions correspondence for existing T2V models. The proposed S²AG-Vid pipeline is illustrated in Fig. 3. Given a text prompt P of length L , we define the set of words in P as $S = \{s_1, s_2, \dots, s_L\}$. We also define the set of noun and verb pairs in P as S^* , $s_i^* = \{s_i, s_j\} \in S^*$ (where, s_i is a noun, s_j is a verb, i and j is respective indices in S). To address issues of *subject count mismatch* and *incorrect motion binding*, we propose spatial-aware and syntax-aware constraints, denoted as \mathcal{L}_{sp} and \mathcal{L}_{syt} , respectively.

3.3.1 Introducing Spatial Position-Based Prior

Based on the **observation 1**, our initial goal is to adjust the CA maps of nouns during the early denoising stages, ensuring that their attention areas become concentrated and distinctly separated from each other. To achieve this, we introduce additional spatial-based priors, i.e., bounding boxes, to quickly guide nouns to focus on specified regions.

Specifically, let $B = \{B_i^f\}$ represent the set of spatial position priors corresponding to nouns in S^* , where B_i^f denotes the spatial position prior of the f -th frame corresponding to the i -th noun in S . Each B_i^f contains top-left and bottom-right coordinates. A set of spatial masks $M = \{M_i^f\}$ is obtained by transforming B , where the value inside the box is 1 and the value outside the box is 0. To ensure that the CA maps of nouns concentrate on regions defined by the given spatial prior, we propose a spatial-aware constraint aimed at enhancing the focus of these CA maps on the foreground object,

$$\mathcal{L}_{ig} = \frac{1}{F} \sum_{i,j \in S^*} \sum_{f \in F} \left(1 - \frac{A_i^f \cdot M_i^f}{A_i^f} \right)^2. \quad (1)$$

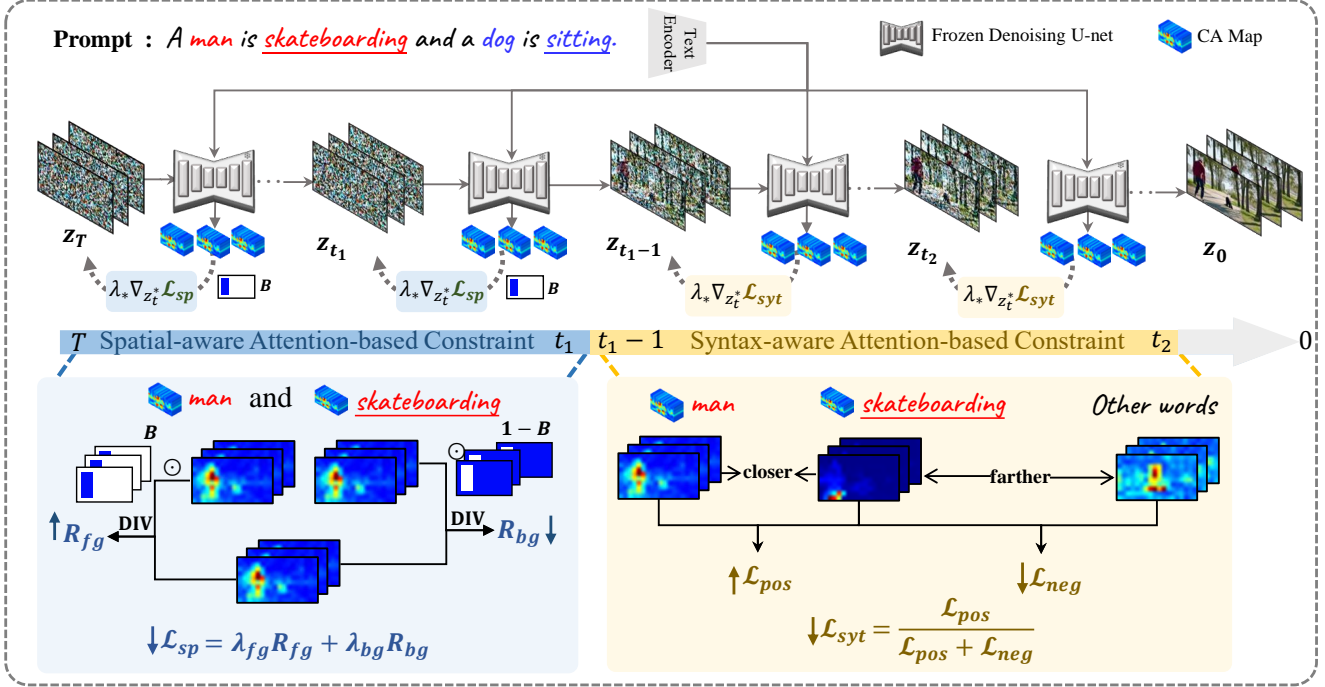


Figure 3. **Illustration of S^2 AG-Vid.** To enhance multiple subject-motion correspondences, we employ spatial and syntactic attention-based guidance on the noise latent feature z_t . In the early denoising step, we construct spatial-aware attention-based constraint \mathcal{L}_{sp} that guides the CA maps of nouns (e.g., “man”) and verbs (e.g., “skateboarding”) to specific spatial locations. In the subsequent denoising phase, we introduce a syntax-aware attention-based constraint \mathcal{L}_{syt} , which minimizes the disparity between the CA maps of verbs (e.g., “skateboarding”) and their associated nouns (e.g., “man”), while simultaneously ensuring their differentiation from other tokens. This reinforcement efficiently strengthens the semantic linkage between subjects and their corresponding motions.

Focusing exclusively on the information within the spatial prior ensures that the subject remains within the specified range; however, it does not prevent nouns from considering information outside the bounding boxes, potentially leading to the generation of multiple subjects outside the designated region. Therefore, we propose an additional background constraint aimed at minimizing the influence of the CA maps of nouns outside the bounding boxes, as follows,

$$\mathcal{L}_{bg} = \frac{1}{F} \sum_{i,j \in S^*} \sum_{f \in F} \left(\frac{A_i^f \cdot (1 - M_i^f)}{A_i^f} \right)^2. \quad (2)$$

Consequently, the overall spatial-aware attention-based constraint can be formulated as,

$$\mathcal{L}_{sp} = \lambda_{fg} \mathcal{L}_{fg} + \lambda_{bg} \mathcal{L}_{bg}. \quad (3)$$

Moreover, considering that the CA maps of verbs A_j^f should mirror those of nouns for motion correspondence, we also apply Eq.(3) to the CA maps of verbs to reinforce this alignment using the same bounding boxes with the corresponding nouns.

3.3.2 Enhanced Motion and Subject Correspondence

Under the spatial constraints applied to both nouns and verbs, the CA maps of verbs can, to some extent, align with the regions defined by the spatial priors. However, a clear relationship between the CA maps of verbs and nouns is still lacking. According to **observation 2**, our goal is to leverage the syntactic relationships to establish a strong connection between verbs and nouns, thereby enhancing the alignment between motion and corresponding subjects. As a result, our approach involves introducing contrastive learning to minimize the distance between the CA map of verbs and that of the corresponding nouns, while simultaneously distancing it from the CA maps of other words to prevent interference.

In particular, we construct a syntax-aware contrastive constraint, where the noun and verb pairs in each s_i^* serve as positive samples for each other, while other words in S act as their negative samples. For the noun s_i and the verb s_j in s_i^* , our positive loss aims to minimize the distance between the CA map of s_i and s_j ,

$$\mathcal{L}_{pos}(s_i^*) = \frac{1}{F} \sum_{f \in F} f_{dist} \left(A_i^f, A_j^f \right), \quad (4)$$

where $f_{dist}(\cdot)$ represents the calculation of the distance function between CA maps. For s_i^* , we define the set of

other words in S as U_i . Our negative loss encourages the separation of i -th word pairs from the words in U_i ,

$$\mathcal{L}_{neg}(s_i^*, U_i) = \frac{1}{F} \sum_{u \in U_i} \sum_{f \in F} f_{dist}(A_i^f, A_u^f). \quad (5)$$

Finally, the syntax-aware attention-based constraint can be formulated as follows,

$$\mathcal{L}_{syt} = \sum_{s_i^* \in S^*} \frac{\mathcal{L}_{pos}(s_i^*)}{\mathcal{L}_{pos}(s_i^*) + \mathcal{L}_{neg}(s_i^*, U_i)}. \quad (6)$$

3.3.3 Performing Latent Guidance

After obtaining the constraints, we compute their gradients to update z_t at each timestep as follows,

$$z'_t \leftarrow z_t - \alpha \cdot \lambda_* \nabla L_*, \quad (7)$$

where α represents the learning rate of the optimization process and λ_* control the weighting of the constraint. Specifically, we initially apply Eq.(3) in the first 5 steps out of 50 denoising steps. The spatial-aware guidance first optimizes z_t to gradually align with the specified spatial prior, accurately generating the correct number of subjects and ensuring that their motions correspond to the positions of the related objects. Subsequently, Eq.(6) is implemented over the next 20 steps to further refine z_t shift, enhancing the high-response attention alignment between nouns and verbs.

4. Experiments

Setup and Baselines. We adopt the open-source T2V generation model, ModelScope [28], as our backbone and apply our method on top of it. Specifically, we employ the model version named Zeroscope. Additionally, we benchmark our approach against the recent model LVD [15], which also uses ModelScope [28] as its backbone. Notably, LVD [15] incorporates an LLM [1] to create dynamic scenes from text prompts, yielding video motions that closely mimic real-life movements. All generated videos are at a resolution of 320×576 and span 16 frames. Our experiments are carried out on a single V100 GPU. Our hyperparameters are set as follows: $t_1 = 5$, $t_2 = 25$. The weights for λ_{fg} and λ_{bg} are both 1, while the loss weight for \mathcal{L}_{sp} and \mathcal{L}_{syt} are 30 and 20, respectively. The learning rate α is fixed as 1. For more detailed information, please refer to Section A.1.

Benchmarks. To validate the effectiveness of our method S²AG-Vid, and to facilitate comparisons with other methodologies, we collect n subjects and m actions using the template “an *object1* is *motion1* and an *object2* is *motion2*” to generate text prompts containing multiple subjects and corresponding motions. By selecting combinations of subjects and motions, we generate a total of 200 prompts. For a detailed description of the dataset, please refer to Section A.2.

Metrics/Method	ZeroScope	LVD [15]	Ours
CLIP-I (↑)	0.95	<u>0.94</u>	0.95
Pick Score(↑)	20.21	<u>20.41</u>	20.45
CLIP-T(↑)	<u>26.28</u>	25.67	27.02

Table 1. **Quantitative comparisons between our.** Bold and underline indicate the best and second best value, respectively.

Following LVD [15], we leverage the powerful capabilities of LLM [1] to generate corresponding bounding boxes from text prompts as spatial priors. Further details on utilizing LLM [1] to generate spatial priors from text prompts are provided in Section A.2.

4.1. Qualitative Comparisons

We qualitatively compare the video frames generated by our proposed method S²AG-Vid, to those produced by the baseline and LVD [15]. As illustrated in Fig. 4, our method ensures the accurate generation of subjects and alignment of their motions with the textual descriptions. In contrast, ModelScope [28] fails to generate the correct number of subjects or properly align their motions. For example, in the first row of Fig. 4, given the text prompt “a boy is walking and a dog is sitting”, ModelScope [28] generates two dogs instead. Additionally, while LVD [15] generates the correct number of subjects, it exhibits significant action leakage. As demonstrated in the second row of Fig. 4, given the prompt “a woman is jumping and a boy is playing guitar”, the boy is also depicted as jumping. In contrast, our method successfully generates a video where the woman is jumping and the boy is playing the guitar.

Furthermore, the video generated by LVD [15] does not adhere to the specified spatial positional prior, as shown in Fig. 5. For instance, when the prompt states “a girl is skateboarding and a kite is flying”, the “girl” produced by LVD [15] remains stationary and fails to follow the designated path from left to right. Compared to LVD [15], our method accurately generates “girl” that moves from left to right.

Moreover, we also present quantitative and qualitative results using another open-source video diffusion model, i.e., VideoCrafter2 [4] as a baseline model in Section C, with additional qualitative results in Section E.

4.2. Quantitative Comparisons

In this section, we evaluate our S²AG-Vid model against the baseline methods using both automatic evaluations and human evaluations.

4.2.1 Automatic Evaluation

Metrics. We validate the video quality and alignment with textual descriptions using three automatic evaluation metrics: (1) Pick-Score [10], which predicts user preferences for model results. (2) CLIP Image Similarity (CLIP-I), which calculates the cosine similarity between all pairs of

https://huggingface.co/cerspense/zeroscope_v2.576w

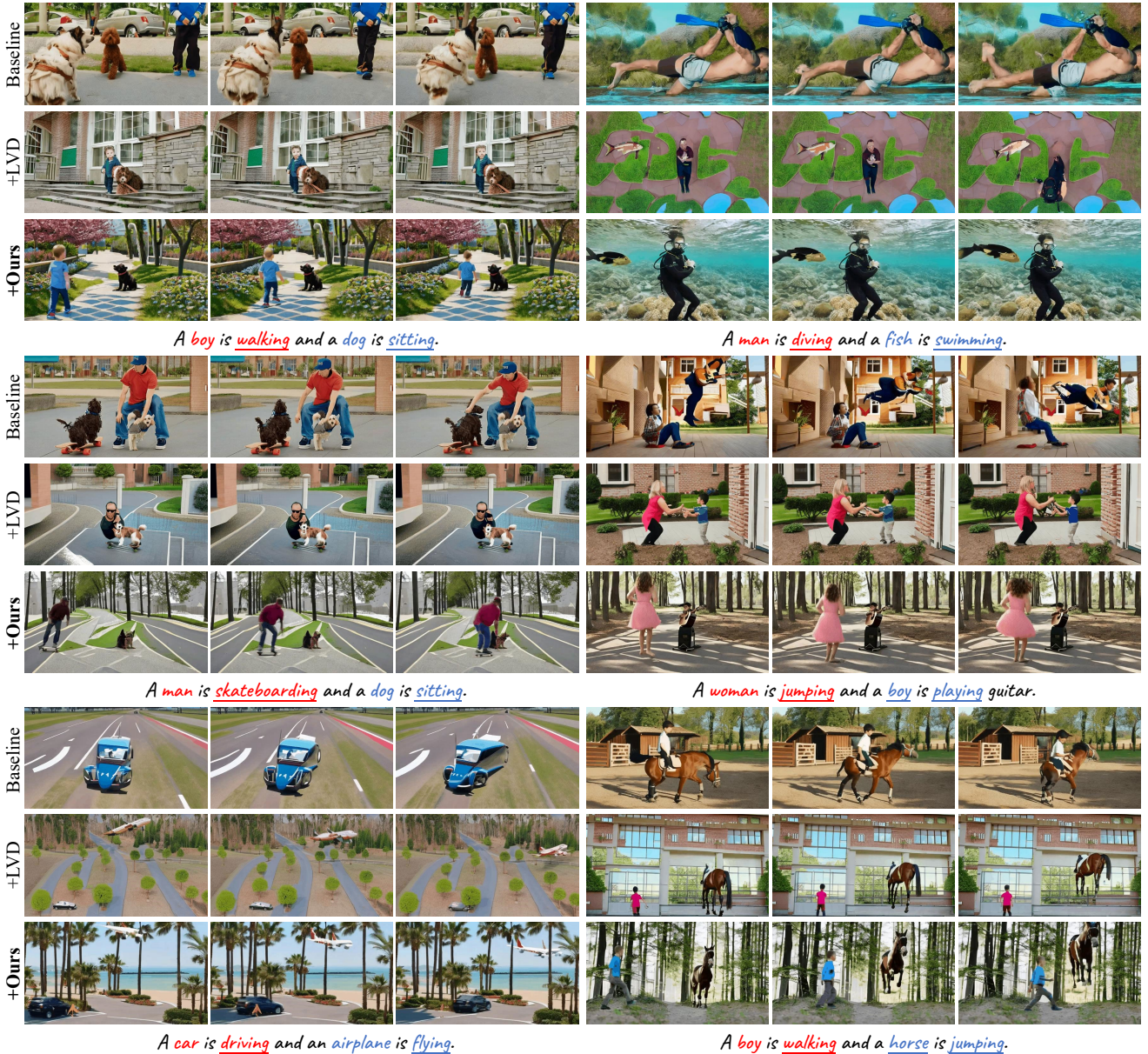


Figure 4. **Qualitative comparisons.** Our proposed S^2AG not only accurately generates the requisite number of subjects but also effectively associates them with their respective motions.

video frames using the CLIP [20] image encoder to assess temporal consistency. (3) CLIP Text Alignment (CLIP-T), which calculates the cosine similarity between video frames and text prompts using the CLIP [20] image encoder and text encoder.

Results. The quantitative results are shown in Table 1. Our S^2AG -Vid outperforms ModelScope [28] and LVD [15] on both CLIP-T and Pick-Score. The results of CLIP-T demonstrate that the outputs produced by my method adhere more closely to the text descriptions. Pick-Score results demonstrate that our outcomes are more favored by users. Additionally, the CLIP-I results indicate that the videos generated by our model exhibit good temporal con-

sistency.

4.2.2 Human Evaluation

We conduct the human-evaluation using Amazon Mechanical Turk (AMT). Specifically, we conduct the user study focusing on two aspects: video quality and video-text alignment. To evaluate the quality of videos, we ask participants three questions: “Which option has the better video quality?”, “Which option is more coherent and smooth?” and “Subjectively, which option do you prefer?”. For video-text alignment, we need participants to answer the following questions regarding the number of subjects and motion alignment: “Which option has the most consistent Number



Figure 5. **Qualitative comparisons between our S²AG and LVD [15].** Although LVD [15] employs bounding boxes as spatial priors, there is a noticeable deviation between the subject’s position and the bounding box in the generated videos. In contrast, our method ensures accurate alignment of the subject within the bounding box.

of subjects with the prompt?” and “Based on the provided prompt, which option is the appropriate Motion for the subjects?”. Complete human evaluator instructions and additional details are provided in Section A.3.

Results. As shown in Fig. 6, human evaluation results indicate that the videos generated by our model significantly outperform those from ModelScope [28] and LVD [15] in both visual quality and alignment with textual descriptions. In terms of human evaluation, the visual effects of the proposed method effectively capture the attention of users, thereby corroborating the results. The proposed method significantly outperforms ModelScope [28] and LVD [15] regarding the number of subjects and the alignment of motion. Specifically, in terms of motion alignment, our method achieves an impressive 94.0% when compared to ModelScope [28], and 92.7% when compared to LVD [15]. This result shows that the proposed method better achieves motion correspondence in multi-subject, multi-motion video generation.

4.3. Ablation Study

We conduct a thorough analysis of the role of different constraints of S²AG-Vid, presenting qualitative results in Fig. 7. Without \mathcal{L}_{sp} , the number of subjects in the result cannot enrich the aligned text description. Without \mathcal{L}_{syt} , the result resembles ours in layout but shows motion leakage, as seen in the third row. Furthermore, without L_{bg} , the result exhibits prior inconsistency within the given bounding boxes. More detailed ablation study can be found in Section B.

	Ours	LVD	Modelscope
Overall Preference	82.0%	18.0%	
Video Fluency	86.7%	13.3%	
Aesthetic Quality	81.3%	18.7%	
Motion Correctness	92.7%	7.3%	
Quantity Correctness	94.0%	6.0%	
			23.3%
			6.7%

Figure 6. **Human preferences in the video generation.** The values displayed indicate the proportion of users who prefer our proposed method over the comparative approach.



Figure 7. **The role of proposed constraint.** \mathcal{L}_{sp} ensures spatial consistency with the bounding box, while the \mathcal{L}_{syt} is crucial for aligning actions with subjects.

5. Conclusions

In this work, we propose a method called S²AG-Vid to generate motion-aligned videos when textual prompts contain multiple subjects with distinct motions. Through observation, we find that adjusting the values of the cross-attention map can modify the subjects’ motions. Consequently, we suggest an untrained method for motion alignment by adjusting the attention maps of nouns and verbs. The effectiveness of our method lies in the initial localization of the CA map’s focus on nouns and verbs, establishing a clear link between nouns and their corresponding verbs. Overall, the proposed method generates videos with accurate motion alignment. Compared to other text-to-video (T2V) generation models, our method demonstrates superior performance in handling multiple subjects and achieving motion alignment.

References

- [1] Josh Achiam, Steven Adler, Sandhini Agarwal, Lama Ahmad, Ilge Akkaya, Florencia Leoni Aleman, Diogo Almeida, Janko Altenschmidt, Sam Altman, Shyamal Anadkat, et al. Gpt-4 technical report. *arXiv preprint arXiv:2303.08774*, 2023. 6, 11
- [2] Hila Chefer, Yuval Alaluf, Yael Vinker, Lior Wolf, and Daniel Cohen-Or. Attend-and-excite: Attention-based semantic guidance for text-to-image diffusion models. *ACM Transactions on Graphics (TOG)*, 42(4):1–10, 2023. 2, 3
- [3] Changgu Chen, Junwei Shu, Lianggangxu Chen, Gaoqi He, Changbo Wang, and Yang Li. Motion-zero: Zero-shot moving object control framework for diffusion-based video generation. *arXiv preprint arXiv:2401.10150*, 2024. 3
- [4] Haoxin Chen, Yong Zhang, Xiaodong Cun, Menghan Xia, Xintao Wang, Chao Weng, and Ying Shan. Videocrafter2: Overcoming data limitations for high-quality video diffusion models. *arXiv preprint arXiv:2401.09047*, 2024. 1, 6, 14, 15
- [5] Minghao Chen, Iro Laina, and Andrea Vedaldi. Training-free layout control with cross-attention guidance. *CoRR*, abs/2304.03373, 2023. 3
- [6] Minghao Chen, Iro Laina, and Andrea Vedaldi. Training-free layout control with cross-attention guidance. In *Proceedings of the IEEE/CVF Winter Conference on Applications of Computer Vision*, pages 5343–5353, 2024. 2, 3
- [7] Tsai-Shien Chen, Chieh Hubert Lin, Hung-Yu Tseng, Tsung-Yi Lin, and Ming-Hsuan Yang. Motion-conditioned diffusion model for controllable video synthesis. *arXiv preprint arXiv:2304.14404*, 2023. 2
- [8] Guillaume Couairon, Marlène Careil, Matthieu Cord, Stéphane Lathuilière, and Jakob Verbeek. Zero-shot spatial layout conditioning for text-to-image diffusion models. In *Proceedings of the IEEE/CVF International Conference on Computer Vision*, pages 2174–2183, 2023. 2, 3
- [9] Weixi Feng, Xuehai He, Tsu-Jui Fu, Varun Jampani, Arjun Akula, Pradyumna Narayana, Sugato Basu, Xin Eric Wang, and William Yang Wang. Training-free structured diffusion guidance for compositional text-to-image synthesis. *arXiv preprint arXiv:2212.05032*, 2022. 4
- [10] Yuwei Guo, Ceyuan Yang, Anyi Rao, Yaohui Wang, Yu Qiao, Dahua Lin, and Bo Dai. Animatediff: Animate your personalized text-to-image diffusion models without specific tuning. *arXiv preprint arXiv:2307.04725*, 2023. 2, 6
- [11] Amir Hertz, Ron Mokady, Jay Tenenbaum, Kfir Aberman, Yael Pritch, and Daniel Cohen-Or. Prompt-to-prompt image editing with cross attention control. *arXiv preprint arXiv:2208.01626*, 2022. 2
- [12] Levon Khachatryan, Andranik Movsisyan, Vahram Tadevosyan, Roberto Henschel, Zhangyang Wang, Shant Navasardyan, and Humphrey Shi. Text2video-zero: Text-to-image diffusion models are zero-shot video generators. In *Proceedings of the IEEE/CVF International Conference on Computer Vision*, pages 15954–15964, 2023. 1, 2
- [13] Yunji Kim, Jiyoung Lee, Jin-Hwa Kim, Jung-Woo Ha, and Jun-Yan Zhu. Dense text-to-image generation with attention modulation. In *Proceedings of the IEEE/CVF International Conference on Computer Vision*, pages 7701–7711, 2023. 2
- [14] Yuheng Li, Haotian Liu, Qingyang Wu, Fangzhou Mu, Jianwei Yang, Jianfeng Gao, Chunyuan Li, and Yong Jae Lee. Gligen: Open-set grounded text-to-image generation. In *Proceedings of the IEEE/CVF Conference on Computer Vision and Pattern Recognition*, pages 22511–22521, 2023. 2
- [15] Long Lian, Baifeng Shi, Adam Yala, Trevor Darrell, and Boyi Li. Llm-grounded video diffusion models. *arXiv preprint arXiv:2309.17444*, 2023. 2, 3, 6, 7, 8, 11, 17, 19, 20, 21, 22, 23
- [16] Han Lin, Abhay Zala, Jaemin Cho, and Mohit Bansal. Videodirectorgpt: Consistent multi-scene video generation via llm-guided planning. *arXiv preprint arXiv:2309.15091*, 2023. 2
- [17] Qi Mao, Lan Chen, Yuchao Gu, Zhen Fang, and Mike Zheng Shou. Mag-edit: Localized image editing in complex scenarios via mask-based attention-adjusted guidance. *arXiv preprint arXiv:2312.11396*, 2023. 3
- [18] William Peebles and Saining Xie. Scalable diffusion models with transformers. In *Proceedings of the IEEE/CVF International Conference on Computer Vision*, pages 4195–4205, 2023. 2
- [19] Quynh Phung, Songwei Ge, and Jia-Bin Huang. Grounded text-to-image synthesis with attention refocusing. *arXiv preprint arXiv:2306.05427*, 2023. 3
- [20] Alec Radford, Jong Wook Kim, Chris Hallacy, Aditya Ramesh, Gabriel Goh, Sandhini Agarwal, Girish Sastry, Amanda Askell, Pamela Mishkin, Jack Clark, et al. Learning transferable visual models from natural language supervision. In *Proceedings of International conference on machine learning*, pages 8748–8763. PMLR, 2021. 7
- [21] Aditya Ramesh, Prafulla Dhariwal, Alex Nichol, Casey Chu, and Mark Chen. Hierarchical text-conditional image generation with clip latents. *arXiv preprint arXiv:2204.06125*, 1(2):3, 2022. 1
- [22] Royi Rassin, Eran Hirsch, Daniel Glickman, Shauli Ravfogel, Yoav Goldberg, and Gal Chechik. Linguistic binding in diffusion models: Enhancing attribute correspondence through attention map alignment. *Advances in Neural Information Processing Systems*, 36, 2024. 3
- [23] Robin Rombach, Andreas Blattmann, Dominik Lorenz, Patrick Esser, and Björn Ommer. High-resolution image synthesis with latent diffusion models. In *Proceedings of the IEEE/CVF conference on computer vision and pattern recognition*, pages 10684–10695, 2022. 1
- [24] Olaf Ronneberger, Philipp Fischer, and Thomas Brox. U-net: Convolutional networks for biomedical image segmentation. In *Medical image computing and computer-assisted intervention—MICCAI 2015: 18th international conference, Munich, Germany, October 5-9, 2015, proceedings, part III 18*, pages 234–241. Springer, 2015. 2
- [25] Chitwan Saharia, William Chan, Saurabh Saxena, Lala Li, Jay Whang, Emily L Denton, Kamyar Ghasemipour, Raphael Gontijo Lopes, Burcu Karagol Ayan, Tim Salimans, et al. Photorealistic text-to-image diffusion models with deep language understanding. *Advances in neural information processing systems*, 35:36479–36494, 2022. 1
- [26] Uriel Singer, Adam Polyak, Thomas Hayes, Xi Yin, Jie An, Songyang Zhang, Qiyuan Hu, Harry Yang, Oron Ashual,

- Oran Gafni, et al. Make-a-video: Text-to-video generation without text-video data. *arXiv preprint arXiv:2209.14792*, 2022. [2](#)
- [27] Jiaming Song, Chenlin Meng, and Stefano Ermon. Denoising diffusion implicit models. *arXiv preprint arXiv:2010.02502*, 2020. [11](#)
- [28] Jiuniu Wang, Hangjie Yuan, Dayou Chen, Yingya Zhang, Xiang Wang, and Shiwei Zhang. Modelscope text-to-video technical report. *arXiv preprint arXiv:2308.06571*, 2023. [1](#), [2](#), [3](#), [4](#), [6](#), [7](#), [8](#)
- [29] Jinheng Xie, Yuexiang Li, Yawen Huang, Haozhe Liu, Wentian Zhang, Yefeng Zheng, and Mike Zheng Shou. Boxdiff: Text-to-image synthesis with training-free box-constrained diffusion. In *Proceedings of the IEEE/CVF International Conference on Computer Vision*, pages 7452–7461, 2023. [2](#), [3](#)
- [30] Shiyuan Yang, Liang Hou, Haibin Huang, Chongyang Ma, Pengfei Wan, Di Zhang, Xiaodong Chen, and Jing Liao. Direct-a-video: Customized video generation with user-directed camera movement and object motion. *arXiv preprint arXiv:2402.03162*, 2024. [2](#)
- [31] Shengming Yin, Chenfei Wu, Jian Liang, Jie Shi, Houqiang Li, Gong Ming, and Nan Duan. Dragnuwa: Fine-grained control in video generation by integrating text, image, and trajectory. *arXiv preprint arXiv:2308.08089*, 2023. [2](#)
- [32] Sihyun Yu, Weili Nie, De-An Huang, Boyi Li, Jinwoo Shin, and Anima Anandkumar. Efficient video diffusion models via content-frame motion-latent decomposition. In *The Twelfth International Conference on Learning Representations*, 2024. [1](#), [2](#)
- [33] Hangjie Yuan, Shiwei Zhang, Xiang Wang, Yujie Wei, Tao Feng, Yining Pan, Yingya Zhang, Ziwei Liu, Samuel Albanie, and Dong Ni. Instructvideo: Instructing video diffusion models with human feedback. *arXiv preprint arXiv:2312.12490*, 2023. [2](#)
- [34] Lvmin Zhang, Anyi Rao, and Maneesh Agrawala. Adding conditional control to text-to-image diffusion models. In *Proceedings of the IEEE/CVF International Conference on Computer Vision*, pages 3836–3847, 2023. [2](#)
- [35] Yabo Zhang, Yuxiang Wei, Dongsheng Jiang, Xiaopeng Zhang, Wangmeng Zuo, and Qi Tian. Controlvideo: Training-free controllable text-to-video generation. *arXiv preprint arXiv:2305.13077*, 2023. [2](#)

Appendix

A. Implementation Details

A.1. Details for Experiments

We introduce our inference settings in this section. We use a DDIM scheduler [27] to perform 50 denoising steps for each generation. For all methods, we generate 16-frame videos with a resolution of 320×576 . In the first 5 steps, we apply L_{sp} guidance 10 times at each time step to ensure the generated subjects conform to the given spatial priors. For L_{syt} , we apply it once at each time step from step 5 to step 25 to align the subjects and their motions. After 25 steps, the model is allowed to automatically adjust the details of the video.

A.2. Details for dataset

We collect a variety of subjects (e.g., boys, women, dogs, cats, balls, vehicles) and actions (e.g., running, standing, flying, skateboarding) commonly featured in video generation. Given that video generation necessitates specific prompts, we eliminate overly abstract subjects and actions, such as “humans” “meditation” and “thinking.” Additionally, we aim to balance authenticity and imagination in video generation. Therefore, we exclude clearly implausible subject-action combinations, such as elephants flying, while retaining feasible ones, such as dogs skateboarding. We then randomly combined the subject-action pairs obtained earlier to generate prompts. These prompts are used alongside ChatGPT-4 [1] to generate bounding boxes [15]. The text prompts and in-context examples are shown in Table 3 and Table 4, respectively. To verify the accuracy of these bounding boxes, we invited 10 volunteers for manual review. Initially, we exclude prompts with conflicting bounding boxes and actions, such as moving bounding boxes paired with sitting actions. Subsequently, we filter out bounding boxes that could degrade the quality of video generation, including those that move too rapidly or significantly exceed the screen boundaries. The dataset categories are as follows:

- **Human Subjects:** Men, Women, Boys, Girls, Robots
- **Animals:** Dogs, Cats, Tigers, Bears, Lions, Elephants, Birds, Horses, Cows, Sheep, Dolphins, Fish
- **Objects:** Footballs, Basketballs, Bicycles, Cars, Motorcycles, Trucks, Tanks, Airplanes, Kites, The Sun, Balloons, Boats
- **Linear Actions:** Running, Walking, Skateboarding, Flying, Sitting, Riding a bicycle, Sailing, Surfing Diving, Swimming, Playing football,
- **Non-Linear Actions:** Jumping, Bouncing, Playing golf, Weightlifting, Riding a horse, Playing the guitar

A.3. Details for user study

We conduct a user study on the Amazon MTurk platform. To assess video quality and video-text alignment separately, we designed two types of questionnaires. Each type of questionnaire consists of over 60 tasks, evaluated by five humans, as depicted in Fig. 8 and Fig. 9. In the video quality evaluation task, participants are presented with a source prompt and two videos generated from this prompt using the same seed. One video is produced by our proposed method, while the other is generated by a randomly selected baseline method. The presentation order of the videos is shuffled to ensure unbiased evaluation. We then pose three questions for the raters to answer:

- Video Quality: Which option has the better video quality?
- Video Fluency: Which option is more coherent and smooth?
- Overall Preference: Subjectively, which option do you prefer?

In the video-text alignment evaluation, the setting and layout of the questionnaire elements remain consistent, with the only variation being the questions themselves. We pose two questions for the raters to answer:

- Number Correctness: Which option has the most consistent Number of subjects with the prompt?
- Motion Correctness: Based on the provided prompt, which option is the appropriate Motion for the subjects?

To ensure the credibility and reliability of our user study, we only involve Amazon MTurk workers with ‘Master’ status and a Human Intelligence Task (HIT) Approval Rate exceeding 90% across all Requesters’ HITs. In total, the 120(60+60) tasks garnered responses from 600 distinct human evaluators.

B. Additional ablation study

B.1. The ablation study of spatial-aware guidance

The impact of time steps in spatial-aware constraints:

We evaluate spatial-aware guidance with 1, 3, 5, and 7 steps between denoising iterations. As illustrated in the Fig. 10, a small number of steps leads to issues with subject count variability, while an excessive number of steps have little effect on the subject’s shape and overall layout. Consequently, we select 5 steps for spatial-aware guidance.

The impact of max-iterations in spatial-aware constraints:

To determine the optimal maximum number of iterations for spatial-aware guidance at each time step, we started with 5 and increased it by increments of 5. As shown in the Fig. 11, a smaller number of iterations led to issues with subject count, while excessive iterations had no significant effect on the shape or overall layout. Therefore, we selected 10 as the maximum number of spatial guidance iterations.

<https://www.mturk.com>

Instructions

This task includes evaluating three AI generated videos in which we provided the same source prompt. Moreover, we hope that the number and the motion of subjects in the generated video are consistent with the prompt. Please view the three videos and provide your feedback on the following criteria:

- **Quality:** Which video has the best generated quality and is most attractive to you?
- **Fluency:** Which video is the most coherent and smooth?
- **Preference:** Subjectively, which video do you prefer?

Question1

Option 1



Option 2



Source Prompt :a airplane is flying and a car is driving

1. Which option has the better video quality?

- Option 1 Option 2

2. Which option is more coherent and smooth?

- Option 1 Option 2

3. Subjectively, which option do you prefer?

- Option 1 Option 2

Figure 8. Example of the video-quality task for 5 human raters on Amazon MTurk to complete.

Instructions

This task includes evaluating three AI generated videos in which we provided the same source prompt. Moreover, we hope that the number and the motion of subjects in the generated video are consistent with the prompt. Please view the three videos and provide your feedback on the following criteria:

- **Number:** Which provides the Number of subjects in the generated video that is most consistent with prompt?
- **Motion:** Which provides the Motion of subjects in the generated video that is most consistent with prompt?

Question1

Option 1



Option 2



Source Prompt :a airplane is flying and a car is driving

1. Which option has the most consistent **Number** of subjects with the prompt?

- Option 1 Option 2

2. Based on the provided prompt, which option is the appropriate **Motion** for the subjects?

- Option 1 Option 2

Figure 9. Example of the video-text alignment task for 5 human raters on Amazon MTurk to complete.



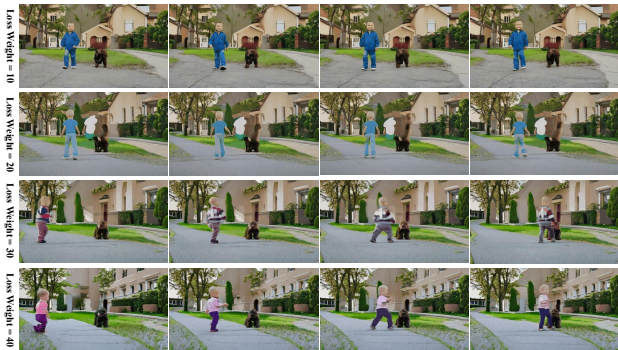
A bird is flying and a dog is walking.

Figure 10. Ablation study of time steps in spatial-aware guidance.



A cat is sitting and a bear is walking.

Figure 11. Ablation study of max-iterations in spatial-aware guidance.



A cat is sitting and a bear is walking.

Figure 12. Ablation study of loss weights in spatial-aware guidance.

The impact of loss weights in spatial-aware constraints:

As illustrated in the Fig. 12, we test spatially guided loss weights in increments of 10, beginning with 10. When the loss weight is too low, it fails to satisfy the spatial prior constraints, potentially leading to issues with the number of subjects. Although loss weights of 30 and 40 yield similar results, we choose a loss weight of 30 for spatial guidance based on practical experience.

B.2. The ablation study of syntax-aware constraints

The impact of time steps in syntax-aware constraints

: To identify the optimal time step for syntax-aware con-



A man is skateboarding and a cat is sitting.

Figure 13. Ablation study of time steps in syntax-aware constraints.



A woman is jumping and a boy is playing-guitar.

Figure 14. Ablation study of max-iterations in syntax-aware constraints.



A man is skateboarding and a boy is riding-bicycle.

Figure 15. Ablation study of loss weights in syntax-aware constraints.

straints, we began with 10 and tested increments of 5. As illustrated in the Fig. 13, fewer time steps result in motion leakage issues (e.g., the cat’s feet constantly moving). Conversely, too many time steps degrade result quality (e.g., the skateboard disappears, the cat appears with multiple tails, and images become blurred). Thus, we select a time step range of 5 to 25 for syntax-aware constraints.

The impact of max-iterations in syntax-aware constraints

: We conduct ablation experiments to determine the optimal maximum number of iterations for syntax-aware constraints at each time step, starting with 1 iteration

method name	CLIP-I (\uparrow)	Pick Score(\uparrow)	CLIP-T(\uparrow)
VideoCrafter2 [4]	0.96	21.20	27.49
Ours	0.96	21.34	28.66

Table 2. **Quantitative comparisons between Ours method and VideoCrafter2 [4].** Bold indicate the best value. and increasing incrementally. As shown in the Fig. 14, a single iteration produces correct results, but additional iterations significantly degrade video quality. 5 Therefore, we select 1 as the maximum number of iterations for syntax-aware constraints.

The impact of loss weights in syntax-aware constraints : We begin with a syntax-aware constraint loss weight of 10 and test increments of 10. As illustrated in the Fig. 15, a low loss weight leads to motion leakage issues. Similarly, a high loss weight also results in motion leakage and negatively impacts video quality. Based on the results, we set the loss weight for syntax-aware constraints to 20.

Selection of distance functions between CA Maps : We use both cosine distance and KL divergence to measure the distance between cross-attention maps (CAMaps). As illustrated in Fig. 16, cosine distance fails to accurately capture movement, while KL divergence effectively measures correct movement. Therefore, we use KL divergence for measuring the distance between cross-attention maps.

Comparison of formulas for syntax-aware constraints : We assess the impact of syntax-aware constraints both with and without contrastive learning. As illustrated in the Fig. 17, without contrastive learning, the straightforward formulation $\mathcal{L}_{pos} + \mathcal{L}_{neg}$ may lead to motion leakage. In contrast, using the formula $\mathcal{L}_{pos}/(\mathcal{L}_{pos} + \mathcal{L}_{neg})$ effectively directs the motion focus towards the intended subject.

B.3. Get CAMap from which layer

We experiment with a low-resolution layer of the diffusion model, which influences the subject’s shape. As shown in Fig. 18, using only up-sampling or down-sampling results in noisy background information, while adding intermediate layers causes subjects to be missing. Combining up-sampling and down-sampling layers yields satisfactory results; thus, we obtain the cross-attention map (CAMap) from the lowest resolution layer that includes both up-sampling and down-sampling.

C. Quantitative and qualitative results of the application on VideoCrafter2

Fig. 19 presents qualitative results using VideoCrafter2 [4] as the baseline model. VideoCrafter2 [4] struggles to generate subjects and motions consistent with the text description, while our method enables it to produce correct motions and subjects. For example, given the text prompt “*a boy is standing and a dog is jumping*”, VideoCrafter2 [4]



Figure 16. Ablation study of distance function.



Figure 17. Comparison of formulas for syntax-aware constraints.



Figure 18. Ablation study of CAMap’s layers.

generates a jumping “*boy*” while the “*dog*” remains still. In contrast, our method successfully generates a video where the “*boy*” is standing and the “*dog*” is jumping.

We quantitatively compare the results on VideoCrafter2 [4]. As illustrated in Table 2, our method outperforms VideoCrafter2 [4] on both CLIP-T and Pick-Score. These results demonstrate that our method enhances VideoCrafter2’s [4] ability to align with text prompts.

D. Limitation

The effectiveness of the proposed method is significantly impacted by the baseline model’s capabilities, leading to time-inconsistent results. This issue arises from limitations in the baseline model ZeroScope. Fig. 21 provides an example of the baseline model’s failure. This issue can be addressed by replacing the baseline model. In Section C, replacing the baseline model with VideoCrafter alleviated the issue.

E. Additional results

In real-world applications, text prompts provided by users are often ambiguous and noisy. Our method employs LLM to automatically parse subjects and motions from text

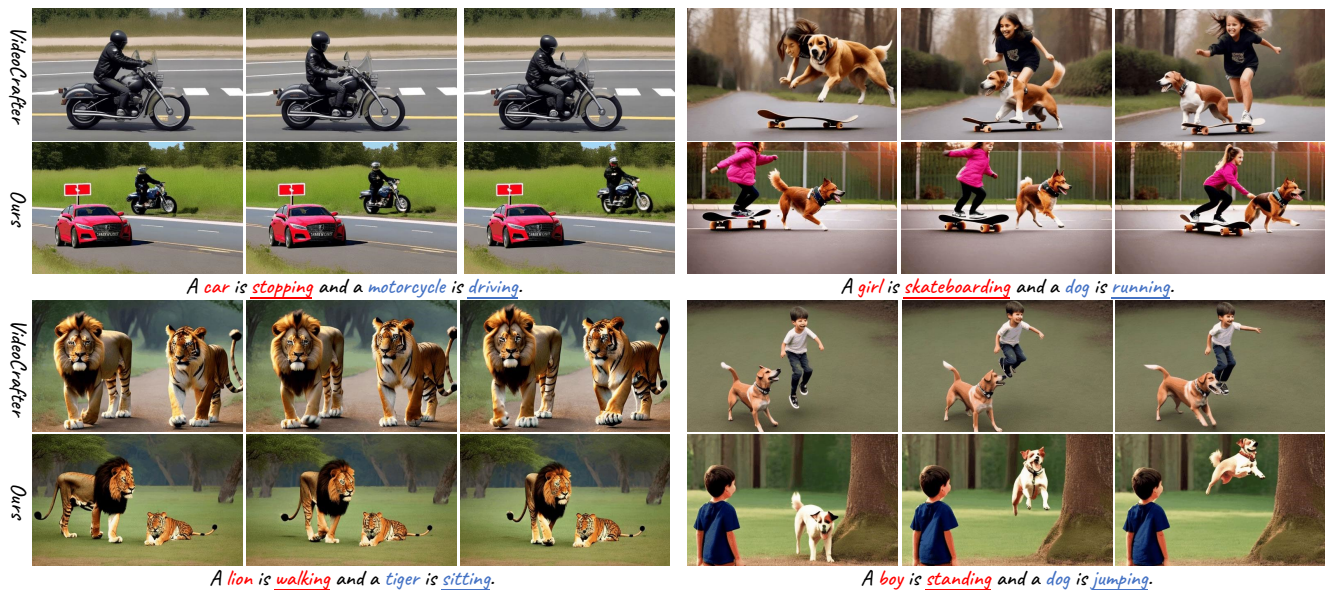


Figure 19. Comparison with VideoCrafter2 [4] and ours methods.

prompts, utilizing the template in Section A.2, and to generate spatial priors accordingly. Fig. 20 illustrates the results for noisy or ambiguous text prompts. Despite the text prompt being blurry and noisy, the proposed method can still generate videos that align with the text prompt.

To assess the impact of the bounding box on the results, we designed various bounding boxes for the same prompt. As shown in Fig. 22, the proposed method consistently generates results that adhere to the spatial prior constraints across different bounding boxes.

Fig. 23 and Fig. 24 illustrates the performance of our method with multiple subjects. Even when the text prompt includes four subjects performing different actions, the proposed method consistently generates high-quality videos.

We present more visual results comparing our method with LVD and Modelscope in Fig. 25 to Fig. 30, further demonstrating the effectiveness of our method in enhancing multi-motion alignment.



Figure 20. Qualitative results of noisy text prompts.



Figure 21. Example of appearance inconsistency in ZeroScope.

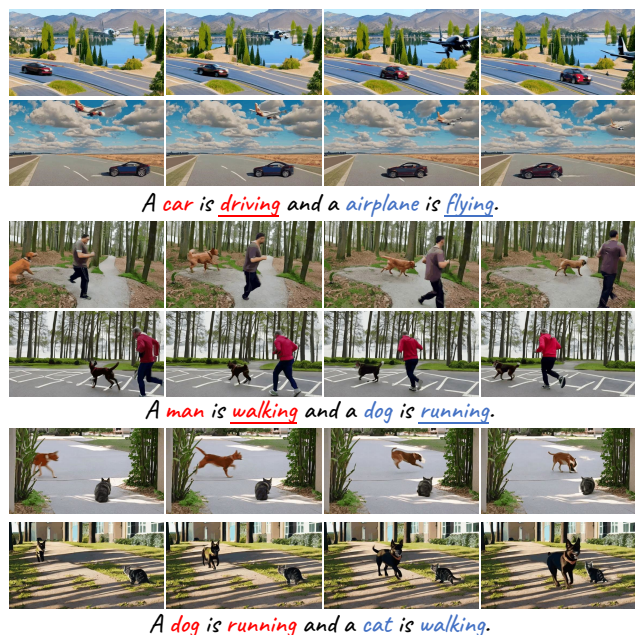


Figure 22. Analysis of the impact of bounding boxes on results.

Table 3. Our prompt for the dataset generation. When using API calls, lines 1-3 presented to GPT-4 with the role “system”. Each caption line in the in-context examples and user query is assigned with role “user”. The example outputs are assigned with the role “assistant”. These lines are merged into one message when querying GPT-4 through the ChatGPT web interface.

```

1 You are an intelligent bounding box generator for videos. You don't need to generate the videos
  themselves but need to generate the bounding boxes. I will provide you with a caption for a video
  with eight frames, with four frames per second. Your task is to generate a list of realistic
  bounding boxes for the objects mentioned in the caption for each frame as well as a background
  keyword. The video frames are of size 320x576. The top-left corner has coordinates [0, 0]. The
  bottom-right corner has coordinnates [573, 320]. The bounding boxes should not overlap or go
  beyond the frame boundaries.
2
3 Each frame should be represented as `[{ 'id': unique object identifier incrementing from 0, 'name':
  object name, 'box': [box top-left x-coordinate, box top-left y-coordinate, box width, box
  height]], ...]`. Each box should not include more than one object. Your generated frames must
  encapsulate the whole scenario depicted by the caption. Assume objects move and interact based on
  real-world physics, considering aspects such as gravity and elasticity. Assume the camera follows
  perspective geometry. Boxes for an object should have the same id across the frames, even if the
  object may disappear and reappear. If needed, you can make reasonable guesses. Provide a concise
  reasoning statement that is not longer than a few sentences before each generation. Refer to the
  examples below for the desired format. Never use markdown or other formats not in the examples. Do
  not start each frame with `'-`. Do not include any comments in your response.
4
5 [In-context examples]
6
7 Caption: {User Text Prompt Generation}
8 Reasoning:

```



Figure 23. Qualitative results with three subjects.



Figure 24. Qualitative results with four subjects.



A woman is running and a car is driving.



A woman is running and an airplane is flying.



A horse is jumping and a car is driving.

Figure 25. Comparison with baseline added with LVD [15] and ours methods.

Table 4. Our in-context examples for the dataset generation. We use these two in-context examples that we use throughout our work unless stated otherwise.

1 Caption: Caption: A woman walking from the left to the right and a man jumping on the right in a room
2 Reasoning: A woman is walking from the left to the right so her x-coordinate should increase with her
y-coordinate fixed. A man is jumping on the right so his x-coordinate should be large, and his
y-coordinate should first decrease (upward movement) and then increase (downward movement due to
gravity).

3 Frame 1: [{'id': 0, 'name': 'walking woman', 'box': [0, 70, 120, 200]}, {'id': 1, 'name': 'jumping
man', 'box': [380, 120, 120, 180]}]
4 Frame 2: [{'id': 0, 'name': 'walking woman', 'box': [35, 70, 120, 200]}, {'id': 1, 'name': 'jumping
man', 'box': [380, 70, 120, 200]}]
5 Frame 3: [{'id': 0, 'name': 'walking woman', 'box': [70, 70, 120, 200]}, {'id': 1, 'name': 'jumping
man', 'box': [380, 30, 120, 200]}]
6 Frame 4: [{'id': 0, 'name': 'walking woman', 'box': [105, 70, 120, 200]}, {'id': 1, 'name': 'jumping
man', 'box': [380, 5, 120, 200]}]
7 Frame 5: [{'id': 0, 'name': 'walking woman', 'box': [140, 70, 120, 200]}, {'id': 1, 'name': 'jumping
man', 'box': [380, 5, 120, 200]}]
8 Frame 6: [{'id': 0, 'name': 'walking woman', 'box': [175, 70, 120, 200]}, {'id': 1, 'name': 'jumping
man', 'box': [380, 30, 120, 200]}]
9 Frame 7: [{'id': 0, 'name': 'walking woman', 'box': [210, 70, 120, 200]}, {'id': 1, 'name': 'jumping
man', 'box': [380, 70, 120, 200]}]
10 Frame 8: [{'id': 0, 'name': 'walking woman', 'box': [245, 70, 120, 200]}, {'id': 1, 'name': 'jumping
man', 'box': [380, 120, 120, 180]}]
11 Background keyword: room
12

13 Caption: A dog is running and a cat is sitting
14 Reasoning: The dog is running, so its position should change across frames. The cat is sitting, so its
position should remain relatively constant across frames.

15
16 Frame 1: [{'id': 0, 'name': 'running dog', 'box': [50, 80, 120, 100]}, {'id': 1, 'name': 'sitting
cat', 'box': [350, 200, 80, 60]}]
17 Frame 2: [{'id': 0, 'name': 'running dog', 'box': [85, 80, 120, 100]}, {'id': 1, 'name': 'sitting
cat', 'box': [350, 200, 80, 60]}]
18 Frame 3: [{'id': 0, 'name': 'running dog', 'box': [120, 80, 120, 100]}, {'id': 1, 'name': 'sitting
cat', 'box': [350, 200, 80, 60]}]
19 Frame 4: [{'id': 0, 'name': 'running dog', 'box': [155, 80, 120, 100]}, {'id': 1, 'name': 'sitting
cat', 'box': [350, 200, 80, 60]}]
20 Frame 5: [{'id': 0, 'name': 'running dog', 'box': [190, 80, 120, 100]}, {'id': 1, 'name': 'sitting
cat', 'box': [350, 200, 80, 60]}]
21 Frame 6: [{'id': 0, 'name': 'running dog', 'box': [225, 80, 120, 100]}, {'id': 1, 'name': 'sitting
cat', 'box': [350, 200, 80, 60]}]
22 Frame 7: [{'id': 0, 'name': 'running dog', 'box': [260, 80, 120, 100]}, {'id': 1, 'name': 'sitting
cat', 'box': [350, 200, 80, 60]}]
23 Frame 8: [{'id': 0, 'name': 'running dog', 'box': [385, 80, 120, 100]}, {'id': 1, 'name': 'sitting
cat', 'box': [350, 200, 80, 60]}]
24 Background keyword: garden



A boy is playing golf and a dog is running.

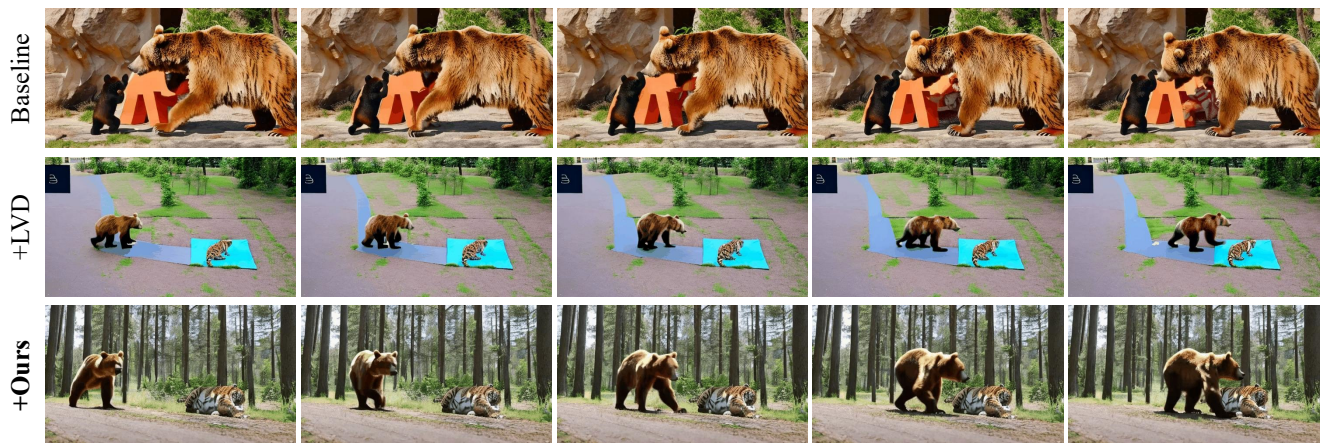


A man is skateboarding and a dog is sitting.

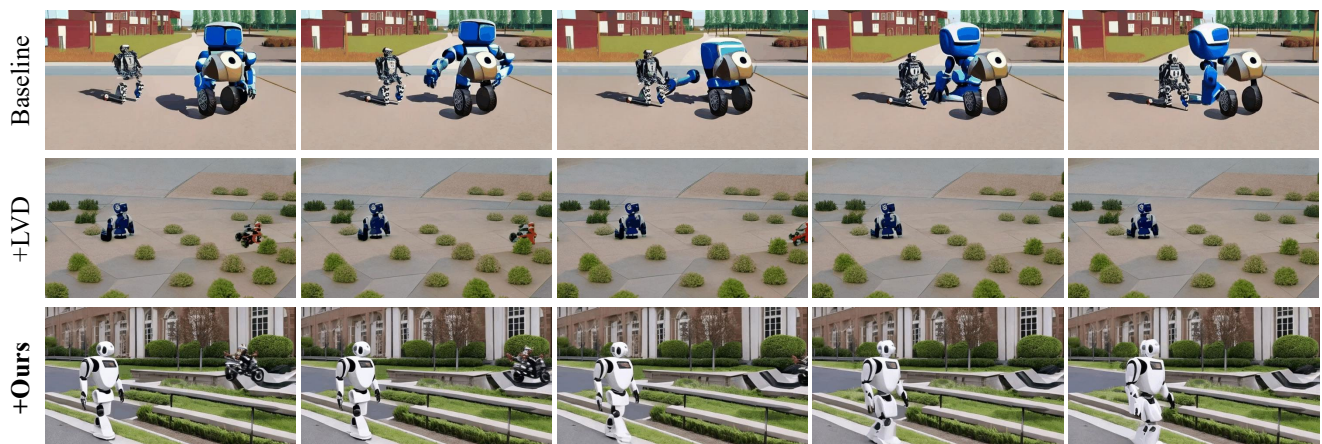


A man is skateboarding and a boy is running.

Figure 26. Comparison with baseline added with LVD [15] and ours methods.



A bear is walking and a tiger is sitting.



A robot is skateboarding and a motorcycle is driving.



A boy is walking and a horse is jumping.

Figure 27. Comparison with baseline added with LVD [15] and ours methods.



An airplane is flying and a car is driving.



A boy is playing guitar and a girl is dancing.

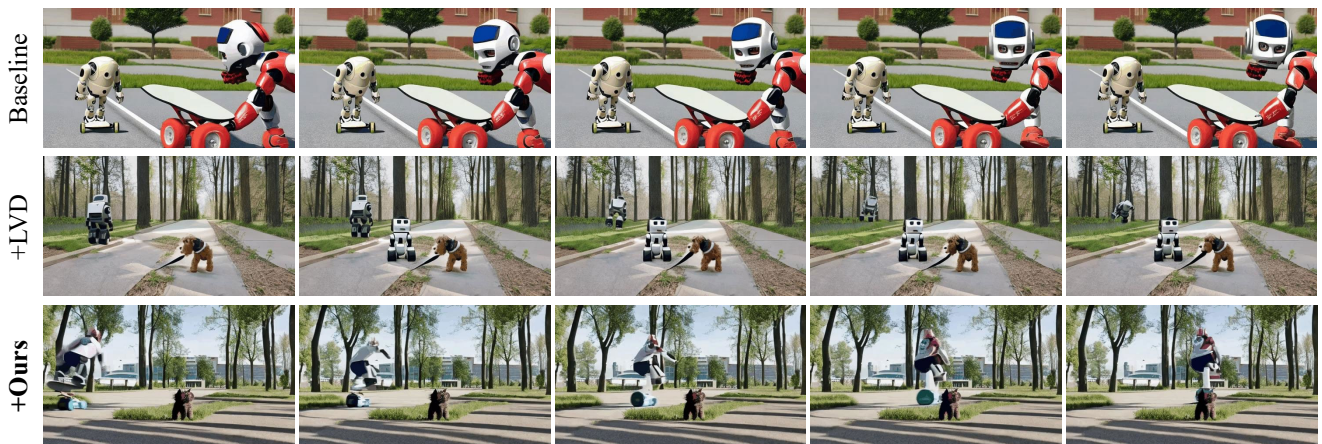


A man is skateboarding and a dog is sitting.

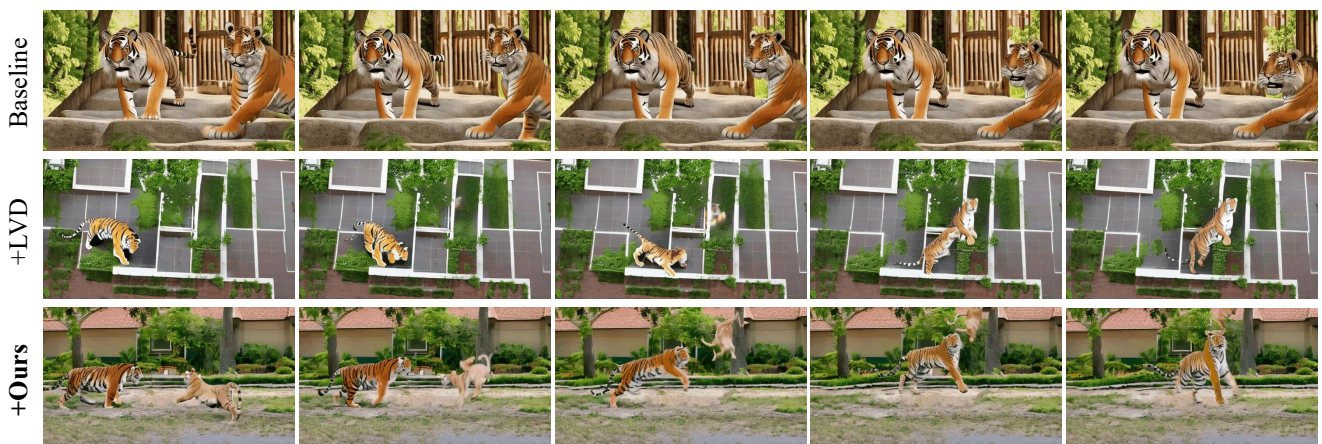
Figure 28. Comparison with baseline added with LVD [15] and ours methods.



A woman is weightlifting and a man is riding horse.



A robot is skateboarding and a dog is sitting.



A tiger is running and a lion is jumping.

Figure 29. Comparison with baseline added with LVD [15] and ours methods.



A girl is running and a kite is flying.



A horse is jumping and a bear is walking.



A man is skateboarding and a boy is jumping.

Figure 30. Comparison with baseline added with LVD [15] and ours methods.